Monohydride and Monofluoride Derivatives of B, Al, N and P. Theoretical Study of Their Ability as Hydrogen Bond Acceptors

Isabel Rozas,*,† Ibon Alkorta,*,‡ and José Elguero

Instituto de Química Médica (CSIC), Juan de la Cierva, 3, 28006-Madrid, Spain

Received: April 26, 1999; In Final Form: July 29, 1999

The characteristics of low-valence derivatives (monohydrides and monofluorides) of boron, aluminum (group 13 of the periodic system), nitrogen, and phosphorus (group 15 of the periodic system) have been investigated. Several aspects of these derivatives have been studied such as the energy gap between their singlet and triplet configuration, their proton affinity in the different parts of the molecule, and their ability as hydrogen bond acceptors. The geometries and energies of all the monomers and complexes have been fully optimized using a hybrid method (B3LYP) and the second-order Møller−Plesset (MP2) levels with the 6-311++G** basis set. In addition, the G2 and MCSCF methodologies were also used. The natural population analysis and the natural bond orbital analysis have been used to evaluate the charge transfer and second-order interaction energies, respectively. Topological properties of the electron density have been characterized using the atoms in molecules methodology. Our results show surprisingly strong hydrogen bonds for the boron derivatives. By use of principal component analysis, it was possible to express the interaction energy as a function of the acidity or basicity and the softness of the molecules involved in the complexes following Pearson's model. As well, it was found, by the natural bond orbital analysis, that the charge is transferred by a $n_{HBA} \rightarrow \sigma^*_{HBD}$ donor−acceptor interaction, similar to standard hydrogen bonds. Moreover, different correlations have been found between the interaction energies and the second-order interaction energies or the charge-transfer calculated for both of the parameters, from the natural bond orbital analysis. The slopes of those correlations vary with the group of the periodic system to which the accepting atom belongs.

Introduction

It is well-known that elements belonging to groups 13−15 of the periodic system (p.s.) can act with two valences, a high and a low one. In most of the compounds formed by these elements they act with the high valence. However, in some important compounds such as carbenes, carbon monoxide, and nitrenes among others, they act with the low valence.[1]

The interest in the low-valence derivatives of boron (BF and BNH_2) has recently increased because of the publication of several articles[2] where the properties of these compounds as organometallic ligands have been compared with other known ligands such as CO and N_2. These theoretical investigations showed that BF and BNH_2 could be excellent ligands. These results open the possibilities of elements belonging to related groups of the p.s. to be able to act as ligands or to establish other noncovalent interactions as acceptors of hydrogen bonds (HB). Thus, aluminum, which belongs to the same group of the p.s. as boron, could behave in a similar way, and derivatives of carbon, silicon, nitrogen, and phosphorus, which are elements located in the next groups of the p.s., could act as good ligands.

In the present study, several aspects of the monohydride and monofluoride derivatives of boron and aluminum (group 13) and nitrogen and phosphorus (group 15) will be treated. This includes the energy gap between their singlet and triplet configuration, their proton affinity in the different parts of the molecule, and their capacity to act as HB acceptors. The study would consider some aspects of the low-valence derivatives of carbon and silicon (group 14), whose ability to form HBs acting as acceptors we have previously investigated.[3] The whole collection of the compounds reported here allows a series of comparisons that we feel are relevant not only in coordination chemistry and in hydrogen-bonded properties but also for general chemists interested in exploring and systematizing the periodic table.

Methods

The geometries of the monomers and the complexes have been fully optimized with the program Gaussian 94[4] using the hybrid method Becke3LYP[5] with the standard 6-31G*[6] and 6-311++G**[7] basis sets and with post-Hartree−Fock second-order Møller−Plesset (MP2)[8] calculations with the largest basis set. In addition, the G2 methodology[9] that incorporates a series of calculations at different levels has been used only for the monomers. For the singlet state of N and P hydrides and fluorides the HOMO and LUMO appear degenerated, so the single-reference-based methods, such as the G2 theory, assign wrong occupation numbers for these orbitals, and for that reason CASSCF(4,3)/6-31G* optimizations[10] have been also carried out for those monomers. The nature of the monomers and complexes as a potential energy minimum has been established at the B3LYP/6-31G*, in all the cases by verifying that all the corresponding frequencies were real.

The interaction energies, E_I(AB), have been calculated as the difference between the energy of the complex and the sum of

* To whom correspondence should be addressed. Fax: 34-91-564 48 53.

† E-mail: rozas@pinar1.csic.es.

‡ E-mail: ibon@pinar1.csic.es.

10.1021/jp991358o CCC: $18.00
Published on Web 10/15/1999

the energies of the monomers,

$$E_I(AB) = E(AB)_{AB} - [E(A)_A + E(B)_B] \quad (1)$$

where $E(AB)_{AB}$ represents the energy of the complex and $E(A)_A$ the energy of the isolated monomer A calculated with its corresponding basis set.

In addition, a corrected interaction energy (E_{I+BSSE}) excluding the inherent basis set superposition error (BSSE) has been evaluated. The BSSE has been calculated using the Boys−Bernardi counterpoise technique[11] and

$$E_{BSSE}(AB) = E(A')_A - E(A')_{AB} + E(B')_B - E(B')_{AB} \quad (2)$$

where $E(A')_{AB}$ represents the energy calculated for monomer A using its geometry in the complex and the complete set of basis functions used to describe the dimer, and $E(A')_A$ is the energy for monomer A using its geometry in the complex and its basis set.

The corrected interaction energies (E_{I+BSSE}) have been calculated with

$$E_{I+BSSE}(AB) = E_I(AB) + E_{BSSE}(AB) \quad (3)$$

The natural population analysis (NPA) and the natural bond orbital (NBO) analysis have been used to evaluate the atomic charges and second-order interaction energies, respectively. Both parameters were used to determine the electronic charge rearrangement that occurs on the formation of the complexes. NPA and NBO calculations have been performed with the NBO code[12] included in Gaussian 94 at the B3LYP level. This method was used, as suggested by Weinhold, because the NBO perturbation analysis is available only when there exists an effective one-electron Hamiltonian to evaluate the orbital energetics (as the Kohn−Sham operator), and no such operator is available at the MP2 level.[13] In the case that one of the monomers of the complexes was a triplet, both α and β spin−orbitals were considered to perform the second-order perturbation analysis.

The topological properties of the electron and energy densities have been characterized using the atoms in molecules methodology (AIM)[14] with the AIMPAC program package[15] at the MP2/6-311++G** level. The AIM methodology self-consistently partitioned any system and its properties into its atomic fragments, considering the gradient vector field of its electron density distribution.

Results and Discussion

Monomers: Ground Electronic State, Geometry, and Energy. It has been experimentally determined that the ground electronic state of BH, BF, AlH, and AlF is $^1\Sigma^+$, whereas that of NH, NF, PH, and PF is $^3\Sigma^+$.[16] In our study, we have computed the energy of both the singlet and the triplet states for the neutral hydrides and fluorides of the atoms in the first two rows of groups 13−15 of the p.s. in their lowest valence (see Table 1).

The computational method used for these calculations was the G2 methodology. However, when one looked at the orbital occupation of the singlet state of the hydrides and fluorides of the atoms of group 15, it is found that in the four molecules the first unoccupied molecular orbital is degenerate with the corresponding HOMO, which is doubly occupied. This is a clear indication that for the four molecules this state is at least a two-configuration state that cannot be properly described by the G2 formalism. For that reason, we decided to carry out MCSCF-(4,3)/6-31G* optimizations of the singlet state of these derivatives of N and P. In the resulting orbital configurations for the four singlets all the occupied MOs have two electrons except for the degenerated HOMO and LUMO, which have one electron each with a singlet arrangement of the spins. These MCSCF calculations were also carried out for the triplets of this set of molecules to determine the relative stability (see Table 1). It is surprising that such a simple CASSCF calculation, which reproduces correctly the configuration state of these molecules, provides total and relative energies very similar to those obtained by using the G2 method, which was not able to properly describe the orbital occupation of this set of monomers (see Table 1).

TABLE 1: Total Energy (au) of the Singlet and Triplet Electronic Configuration and Singlet−Triplet Gap (ΔE, kcal/mol) Calculated at the G2 (MP2(Full)/6-31G*) and CASSCF(4,3)/6-31G* Levels and Experimental Bond Distances (Å)

	energy of the singlet	energy of the triplet	ΔE[a]	bond distance	exptl bond distance[b]
BH	−25.233 970	−25.180 296	33.68	(s) 1.233	1.247
				(t) 1.186	
BF	−124.523 016	−124.386 204	85.85	(s) 1.279	1.267
				(t) 1.329	
AlH	−242.546 191	−242.472 087	46.50	(s) 1.659	
				(t) 1.598	
AlF	−341.821 261	−341.695 808	78.72	(s) 1.671	1.658
				(t) 1.673	
CH_2	−39.058 396	−39.069 013	−6.66	(s) 1.109	
				(t) 1.077	
CF_2	−237.458 832	−237.364 884	58.95	(s) 1.313	
				(t) 1.327	
SiH_2	−290.167 709	−290.130 495	23.35	(s) 1.518	
				(t) 1.481	
SiF_2	−488.664 591	−488.543 015	76.29	(s) 1.616	
				(t) 1.617	
NH	−55.077 651	−55.142 172	−40.49	(s) 1.038	1.045
	−54.883 609[c]	−54.952 356[c]	−43.14[c]	1.020[c]	
				(t) 1.039	
				1.021§	
NF	−154.210 656	−154.272 018	−38.51	(s) 1.310	1.321
	−153.704 696[c]	−153.768 806[c]	−40.23[c]	1.285[c]	
				(t) 1.329	
				1.304[c]	
PH	−341.389 527	−341.428 438	−24.42	(s) 1.424	1.433
	−341.212 610[c]	−341.259 107[c]	−29.18[c]	1.411[c]	
				(t) 1.426	
				1.412[c]	
PF	−440.579 597	−440.618 616	−24.49	(s) 1.614	
	−440.092 781[c]	−440.138 481[c]	−28.68[c]	1.591[c]	
				(t) 1.620	
				1.595[c]	

[a] Positive values of ΔE indicate that the singlet is more stable than the triplet. [b] Harmony, M. D.; Laurie, V. W.; Kuczkowski, R. L.; Schwendeman, R. H.; Ramsay, D. A.; Lovas, F. J.; Lafferty, W. J.; Maki, A. G. *J. Phys. Chem. Ref. Data* **1979**, *8*, 619. [c] Calculated at the CASSCF(4,3)/6-31G* level.

Overall, the hydrides or fluorides of the atoms of group 13 are the ones with more positive singlet−triplet gap and those of group 15 correspond to negative gaps. In other words, the hydrides and fluorides of the atoms of this group 15 are triplets in their ground state. For the molecules with atoms of the 13 and 14 groups, the gaps in the fluorine derivatives tend to be more positive, favoring the singlet configuration. These results are in agreement with the experimental data[16] and with previous computational reports.[17]

In general, the energy differences between singlet and triplet are so large, with the exception of CH_2, that only one of the two species will be present (singlet for the derivatives of B, Al, Si, and CF_2 and triplet for those of N and P). This species would be the ones considered for the present study. In the case

TABLE 2: Total Energy (E_T, au) and Protonation Energy (E_{prot}, kcal/mol) of the Protonated Species Calculated at the G2 Level

	E_T	$E_{prot.}$
HBH^+ (s)	−25.556 763	−202.56
HBF^+ (s)	−124.804 702	−176.76
BFH^+ (s)	−124.682 092	−99.82
$HAlH^+$ (s)	−242.859 459	−196.58
$HAlF^+$ (s)	−342.086 932	−166.71
$AlFH^+$ (s)	−342.083 965	−164.85
HCH_2^+ (s)	−39.385 584	−205.31
HCH_2^+ (t)	−39.252 106	−114.89
HCF_2^+ (s)	−237.738 778	−175.67
CF_2H^+ (s)	−237.667 417	−130.89
$HSiH_2^+$ (s)	−290.477 641	−194.49
$HSiF_2^+$ (s)	−488.919 251	−159.80
SiF_2H^+ (s)	−488.893 913	−143.90
HNH^+ (t)	−55.378 342	−148.20
HNF^+ (t)	−154.449 541	−111.40
NFH^+ (t)	−154.428 981	−98.50
HPH^+ (t)	−341.659 474	−144.98
HPF^+ (t)	−440.821 859	−127.54
PFH^+ (t)	−440.830 519	−132.97

of CH_2, the computed energy difference is quite small (−6.66 kcal/mol) and in favor of the triplet, which is in agreement with the experimental result.[18] The monofluoride derivatives of groups 13 and 14 tend to stabilize the singlet configuration when compared to the corresponding monohydrides. In the case of the derivatives of group 15, almost no differences are observed between monohydrides and monofluorides.

Within the G2 formalism the geometry optimization reaches the level of MP2(Full)/6-31G*. These optimized geometries will be referred in this article as G2 geometries (bonds and angles). The G2, MCSCF, and experimental bond distances of all the monomers studied in their different electronic states are shown in Table 1. In general, the bond distances are shorter in the triplet monohydrides than in their corresponding singlets, whereas the opposite is observed in the case of monofluorides. Some limit cases have been observed, as is the case of NH, PH, and PF where the bond distances are very similar in both configurations. A good agreement has been found between calculated and experimental distances. Thus, when the singlet is more stable than the triplet, the calculated distances of the singlet species are more similar to the experimental results. Similarly, when the triplet is the more stable state, the calculated distance of the triplet is more like the experimental value.

Proton Affinity. The gain in stability due to the protonation of the most stable electronic configuration of all these species (E_{prot}, kcal/mol) was evaluated at the G2 level, and the results are shown in Table 2. The fluoride derivatives (XF; X= B, Al, C, Si, N, and P), similar to the CO molecule, are able to suffer the attack of a proton by both extremes of the molecules.[19] Therefore, both approaches have been taken into account (see Table 2).

In all cases, a large stabilization is observed as a consequence of the protonation (from 98.5 to 205.3 kcal/mol). The protonation energy is larger in the hydrides than in the fluorides. The largest protonation energy is that of the CH_2 molecule (205.31 kcal/mol), which is almost as large as that of the BH molecule (202.56 kcal/mol). The increase in stability of the BF molecule (by the boron extreme, 176.76 kcal/mol) is the largest of all the fluoride species. Generally, all these XF derivatives are better proton acceptors by the X extreme than by the fluorine atom, resulting in larger protonation energies except for the PF molecule (see Table 2). Overall, hydrides and fluorides of atoms in the first two rows of groups 13−15 of the p.s. can be considered bases of medium strength in the gas phase when compared with the experimental protonation affinities of ammonia (204.01 kcal/mol) and water (165.15 kcal/mol).

Regarding the multiplicity of the protonated molecules, it corresponds to that of the more stable configuration of the neutral species (see Table 1) and not necessarily to the most stable cation. Thus, the relative stability of both protonated states (singlet and triplet) was evaluated for the protonated species of NH, NF, PH, and PF, finding that only in the cases of $[HNH]^+$, $[HFN]^+$, and $[HFP]^+$ the multiplicity of the most stable cation was the same as that of the most stable neutral molecule with a singlet−triplet energy gap of −27.85, −41.41, and −24.87 kcal/mol, respectively. However, the multiplicity changed for the most stable protonated species in the case of $[HNF]^+$, $[HPH]^+$, and $[HPF]^+$ (energy gap singlet−triplet: 8.75, 20.32, 43.18 kcal/mol). In the case of CH_2, both singlet and triplet protonated species ($[HCH_2]^+$) were computed, indicating that the most stable was the singlet state with a difference in energy of 83.76 kcal/mol (see Table 2).

Hydrogen-bonded complexes can be considered as intermediates in the protonation process. Thus, the gas-phase basicity of a molecule (that means its stability as a protonated species) could indicate the ability of that molecule to behave as a HB acceptor (more on this topic will be discussed later).

Hydrogen-Bonded Complexes: Geometry and Energy. The complexes formed by the hydrides and fluorides of the atoms of the first two rows of groups 13 and 15 with a set of three HB donors have been computed. As previously mentioned, the fluoride derivatives can act as HB acceptors for both extremes of the molecule. Therefore, both approaches have been considered, and subsequently, these molecules will be treated as different ones (i.e., XF ≠ FX within a HB complex). Hydrogen fluoride, hydrogen cyanide, and hydrogen isocyanide have been used as HB donors.

It was impossible to obtain, at any level of theory, any HB complex with PF when the phosphorus acts as acceptor, and the systems obtained were bounded by other types of interactions (CNH···PF evolved to CNH···FP; FH···PF evolved to HF··· PF; and NCH···PF evolved to HCN···PF). At the MP2/6-311++G** level, most of the HB complexes calculated are linear with the exception of those complexes with NF, PH, FN, and FP, which show H···X−Y angles between 155.5° and 125.5°. At the same level of theory, the A−H distances of the HB donors are very similar to those of the isolated monomers, whereas the HB acceptors become more deformed (longer X−Y distances) if the acceptor atom is a fluoride. In general, and taking into account the atomic radius of the HB acceptor atom, all the complexes show H···X (X = F, B, Al, N, P) distances within the range of a HB interaction (see Table 3). For example, in the case of the complexes were the acceptor is B, N, or F (first row of the p.s.) the H···X distances are 1.731 Å for FH···FAl and 2.708 Å for NCH···BF. In contrast, all the complexes with AlH, PH, and AlF show H···X distances very large (ranging from 2.705 to 3.409 Å; see Table 3), which is a consequence of the large atomic radius of these second-row elements. In the case of the Si derivatives, the H···Si distances previously obtained were 2.488 Å for $FH\cdots SiH_2$ and 2.961 Å for $NCH\cdots SiH_2$.[3]

In terms of energy, we will comment on only those results with the largest basis set (B3LYP/6-311++G** and MP2/6-311++G**), which are shown in Table 3. In this table, we have gathered both the interaction energy and that corrected by the BSSE effect. It is observed that when the BSSE is taken into account, some positive interaction energies result. This gives

TABLE 3: Interaction Energies Without (E_I) and With the BSSE Correction (E_{I+BSSE}, kcal/mol) and H···X Distances (Å)

	B3LYP/6-311++G**		MP2/6-311++G**		
	E_I	E_{I+BSSE}	E_I	E_{I+BSSE}	d(H···X)
FH···BH (s)	−10.23	−9.91	−8.71	−7.99	2.040
FH···BF (s)	−6.23	−5.88	−5.22	−4.62	2.148
FH···FB (s)	−0.69	−0.40	−0.77	−0.29	2.235
NCH···BH (s)	−4.42	−4.23	−4.47	−3.96	2.622
NCH···BF (s)	−2.54	−2.41	−2.82	−2.44	2.708
NCH···FB (s)	−0.18	0.00	−0.52	−0.09	2.512
CNH···BH (s)	−7.46	−7.24	−7.91	−7.24	2.229
CNH···BF (s)	−4.39	−4.18	−4.86	−4.32	2.545
CNH···FB (s)	−0.45	−0.23	−0.90	−0.38	2.272
FH···AlH (s)	−4.96	−4.68	−4.21	−3.53	2.705
FH···AlF (s)	−1.52	−1.23	−1.34	−0.87	2.948
FH···FAl (s)	−9.09	−8.25	−8.37	−7.10	1.731
NCH···AlH (s)	−1.93	−1.75	−2.43	−1.91	3.189
NCH···AlF (s)	−0.14	0.04	−0.68	−0.32	3.409
NCH···FAl (s)	−5.86	−5.33	−5.68	−4.81	2.008
CNH···AlH (s)	−3.36	−3.15	−4.16	−3.51	2.852
CNH···AlF (s)	−0.62	−0.42	−1.31	−0.88	3.050
CNH···FAl (s)	−8.38	−7.73	−8.69	−7.52	1.786
FH···NH (t)	−6.16	−5.84	−5.83	−5.10	1.927
FH···NF (t)	−1.17	−0.84	−1.06	−0.47	2.345
FH···FN (t)	−1.04	−0.76	−1.41	−0.80	2.123
NCH···NH (t)	−3.34	−3.19	−3.58	−3.11	2.324
NCH···NF (t)	−0.41	−0.24	−0.77	−0.31	2.623
NCH···FN (t)	−0.46	−0.25	−1.01	−0.44	2.430
CNH···NH (t)	−5.16	−4.94	−5.80	−5.10	2.191
CNH···NF (t)	−0.77	−0.56	−1.06	−0.52	2.389
CNH···FN (t)	−0.79	−0.58	−1.57	−0.89	2.157
FH···PH (t)	−1.47	−1.22	−1.77	−0.75	2.708
FH···FP (t)	−4.49	−3.77	−5.02	−3.53	1.835
NCH···PH (t)	−0.56	−0.42	−1.36	−0.53	4.051
NCH···FP (t)	−2.88	−2.43	−3.55	−2.49	2.108
CNH···PH (t)	−0.98	−0.82	−1.93	−0.97	2.735
CNH···FP (t)	−4.12	−3.50	−5.37	−3.88	1.890

evidence to the problem that the inclusion of this effect has on weak interactions such as weak HBs or van der Waals interactions in general.[20] The most stable complexes (highest interaction energies in absolute value) are those formed by FH and CNH as HB donors. Independently of the nature of the HB donor, a general trend is observed in the stability of the complexes. Thus, the HB acceptors (considered as X−Y in the A−H···X−Y complexes) can be classified into three groups. First, the most stable complexes are those formed with BH, BF, NH, FAl, and FP. They show E_{I+BSSE}s corresponding to weak HBs (between −12.0 and −2.4 kcal/mol[21]) at the B3LYP level as well as at the MP2 level (B3LYP, between −9.9 and −2.4 kcal/mol; MP2, between −8.0 and −2.4 kcal/mol; see Table 3). Second, are those complexes formed with AlH in which, depending on the HB donor, the E_{I+BSSE}s correspond to a weak HB or to an even weaker interaction (less than −2.4 kcal/mol), henceforth termed in this paper as a van der Waals interaction (B3LYP, between −4.7 and −1.7 kcal/mol; MP2, between −3.5 and −1.9 kcal/mol; see Table 3). The third group is formed by NF, PH, AlF, FB, and FN, which formed the less stable complexes. When taking into account their E_{I+BSSE}s, these can be considered as van der Waals interactions (B3LYP, between −1.2 and 0.0 kcal/mol; MP2, between −1.0 and −0.1 kcal/mol; see Table 3). In Figure 1 we have represented the interaction energy of all the HB complexes (E_I and E_{I+BSSE} in kcal/mol) calculated at the MP2 level vs the different bases, and the three groups already mentioned are easily differentiated in both graphs.

Pearson's Analysis of Interaction Energies (E_I). Pearson's analysis of classical (i.e., proton transfer) acidity and basicity has the form of eq 4 where S is a measure of the strength of the

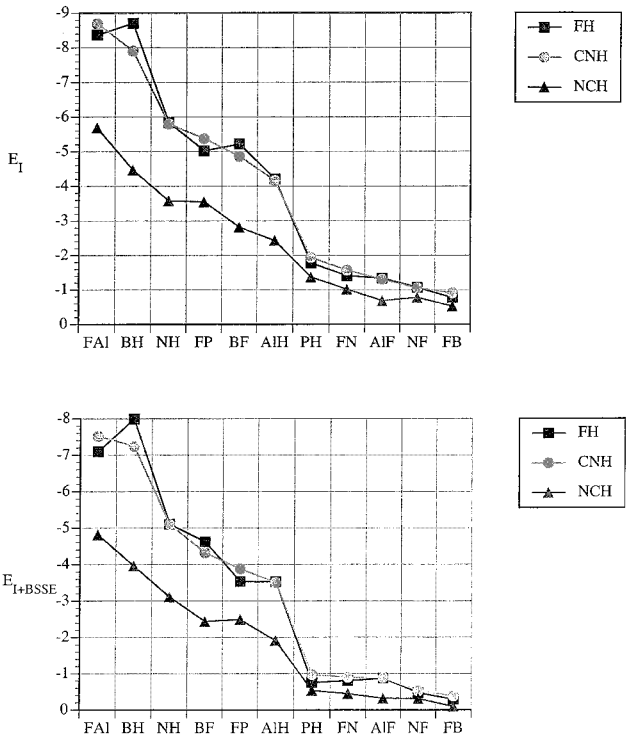

Figure 1. Interaction energy of all the HB complexes (E_I and E_{I+BSSE}, kcal/mol) calculated at the MP2 level vs the different bases.

acid AH or the base XY and σ_{AH} and σ_{XY} are measures of some characteristic different from strength, called "softness".[22] We have computed the E_Is at the MP2 level for all combinations of the 3 acids and 11 bases (3 × 11 matrix). To analyze the dependence of these 33 E_Is with some individual properties of the acids A−H and the bases X−Y, principal component analysis (PCA) offers the best unbiased approach because it is not necessary to make any assumption or to give an arbitrary value to one of the parameters. The result of the PCA shows that the E_Is can be expressed using Pearson's model (eq 5) but with HB donor or acceptor properties instead of thermodynamic

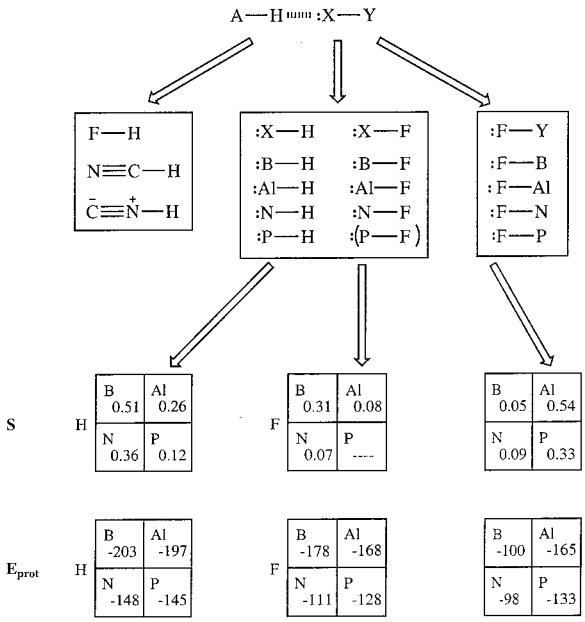

Figure 2. Diagrams of HB strength (S_{XY}) of bases vs protonation energies (E_{prot}).

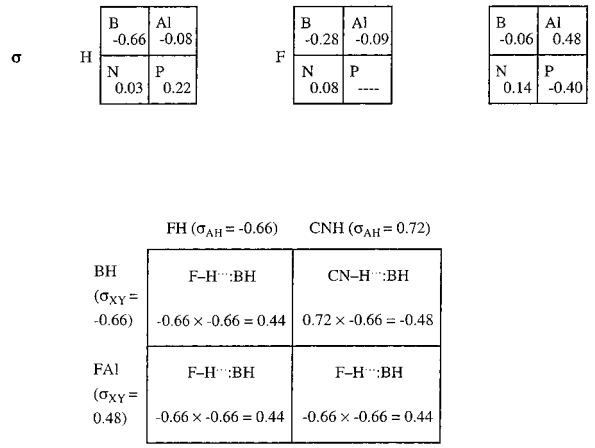

Figure 3. Diagrams of softness of bases (σ_{XY}) and the four most important interactions.

TABLE 4: Matrices Related through X = ABC′ (C′ Is the Transpose of C)

	[,1]	[,2]	[,3]
X (Data)			
[1,]	8.7057	4.4657	7.9059
[2,]	5.2172	2.8198	4.8581
[3,]	0.7729	0.5225	0.9051
[4,]	4.2095	2.4315	4.1629
[5,]	1.3362	0.6808	1.3056
[6,]	8.3667	5.6852	8.6919
[7,]	5.8337	3.5811	5.7969
[8,]	1.0626	0.7741	1.0565
[9,]	1.4058	1.0117	1.5689
[10,]	1.7739	1.3647	1.9323
[11,]	5.0245	3.5509	5.3714

Decomposition into Singular Values: Obtention of Three Matrices

	[,1]	[,2]	[,3]
	A (Principal Components)		
[1,]	0.51076834	−0.66217995	0.17261261
[2,]	0.31156500	−0.28071880	0.07034705
[3,]	0.05270877	0.06300079	−0.46185879
[4,]	0.26028492	−0.07723402	−0.49417590
[5,]	0.08073763	−0.08585005	−0.41296869
[6,]	0.54204745	0.47574432	0.17866074
[7,]	0.36485388	0.03362070	−0.04893251
[8,]	0.06843902	0.08402743	0.42811075
[9,]	0.09483160	0.13803496	−0.26371138
[10,]	0.11984109	0.22079265	0.20277887
[11,]	0.33170065	0.40383609	−0.09451900
	B (Eigenvalues)		
[1,]	24.58488	0.000000	0.0000000
[2,]	0.00000	1.121467	0.0000000
[3,]	0.00000	0.000000	0.1590544
	C (Principal Axes)		
[1,]	0.6534599	−0.6596924	0.3712089
[2,]	0.3967238	0.7161174	0.5742700
[3,]	0.6446707	0.2279950	−0.7296697

acidity and basicity.

$$E_I = a(S_{AH}S_{XY}) + b(\sigma_{AH}\sigma_{XY}) \quad (4)$$

$$E_I = 24.58(S_{AH}S_{XY}) + 1.21(\sigma_{AH}\sigma_{XY}) \quad (5)$$

a and b are the eigenvalues, S_{XY} and σ_{XY} the first two principal components, and S_{AH} and σ_{AH} the first two principal axes. All the values obtained for components and axes are given in Table 4. The coefficients of eq 5, 24.58 and 1.21, reflect the different weights of S and σ. Therefore, it is expected that S is to be related to the acidity and the basicity (proton transfer) but only in the loose way that thermodynamic equilibria are related to HBs. Hydrogen fluoride (S_{AH} = 0.653) and hydrogen cyanide (S_{AH} = 0.645) are much stronger than hydrogen isocyanide (S_{AH} = 0.397). To discuss the HB basicity, S_{XY}, we have used a series of diagrams (Figure 2) where S_{XY} is compared with E_{prot} (Table 2). As expected, there is a rough parallelism with frequent but small inversions. It thus seems justified to assimilate S, as obtained from PCA, to the HB strengths of AH and XY.

If the model were truncated here [E_I = 24.58 ($S_{AH}S_{XY}$)], almost all (99.755%) of the variance would be explained; the addition of the second term [1.21 ($\sigma_{AH}\sigma_{XY}$)] only increases the variance to 99.995%.

Let us consider, for instance, the four extreme cases represented in Figure 3. It shows that if both are of the same sign, the AH−XY interaction will be positive (i.e., E_I will increase), while if both are of different sign, the interaction will be negative, i.e., decreasing E_I. This explains the crossing observed in Figure 1 (top left).

Legon described in 1987[23] a model containing only the first term of eq 4, $k_\sigma = cN_BE_{HX}$, where k_σ is the experimental HB stretching force constant, N_B the nucleophilicity of the proton acceptor (which should correspond to S_{YZ}), and E_{HX} the electrophilicity of the proton donor (which should correspond to S_{AH}). It is not possible to further discuss Pearson and Legon's models because our set of bases is rather unconventional.

Natural Population and Natural Bond Orbital Analyses. The NP and NBO analyses were carried out at the B3LYP/6-311++G** level to evaluate the charge transferred in the formation of the complex and the second-order interactions (energies and nature of the interactions). The results obtained are shown in Table 5 (for complexes that are singlets) and in Table 6 (for complexes that are triplets). Second-order interaction energies are calculated by the equation

$$\Delta E_{ij}^{(2)} = \frac{2F_{ij}^2}{E_i - E_j} \quad (6)$$

where $F_{ij} = \langle\phi_i|F|\phi_j\rangle$, F being the Fock operator, and E_i and E_j are the orbital energies of the donor ϕ_i and acceptor ϕ_j natural bond orbitals.[24]

TABLE 5: NPA Charge Transferred (ΔQ) and NBO Second-Order Interaction Energy ($\Delta E_{ij}^{(2)}$) for the Corresponding Donor−Acceptor Interactions ($n_{HBA} \rightarrow \sigma^*_{HBD}$) of the Singlet Complexes Calculated at the B3LYP/6-311++G Level**

	ΔQ (e)	$\Delta E_{ij}^{(2)}$ (kcal/mol)	$E_j - E_i$ (au)	F_{ij} (au)
FH···BH	0.149	37.56	0.74	0.150
FH···BF	0.085	25.43	0.75	0.124
FH···FB	0.001	0.43	1.51	0.023
NCH···BH	0.050	10.25	0.79	0.080
NCH···BF	0.030	6.75	0.76	0.063
NCH···FB	0.002	0.71	1.47	0.029
CNH···BH	0.105	22.70	0.80	0.121
CNH···BF	0.061	14.63	0.79	0.096
CNH···FB	0.003	1.04	1.50	0.035
FH···AlH	0.068	13.97	0.72	0.090
FH···AlF	0.031	7.29	0.71	0.064
FH···FAl	0.020	6.83	1.56	0.092
NCH···AlH	0.028	4.76	0.72	0.052
NCH···AlF	0.011	1.73	0.68	0.031
NCH···FAl	0.013	5.55	1.50	0.082
CNH···AlH	0.054	9.18	0.74	0.074
CNH···AlF	0.026	4.37	0.72	0.050
CNH···FAl	0.023	8.26	1.56	0.102

TABLE 6: NPA Charge Transferred and NBO Second-Order Interaction Energy (kcal/mol) for the Corresponding Donor−Acceptor Interactions ($n_{HBA} \rightarrow \sigma^*_{HBD}$) of the Triplet Complexes Calculated at the B3LYP/6-311++G Level and HXY Angles at That Level of Calculation**

	ΔQ (*e*)	$\Delta E_{ij}^{(2)}$ (kcal/mol)	$E_j - E_i$ (au)	F_{ij} (au)	*a*(HXY) (deg)
FH···NH (t)	0.029	α: 3.90	1.23	0.088	180.0
		β: 5.87	1.09	0.101	
FH···NF (t)	0.006	α: 1.69	0.88	0.049	133.4
		β: 0.82	1.09	0.038	
FH···FN (t)	0.003	α: 0.68	1.04	0.033	128.5
		β: 0.57	0.91	0.030	
NCH···NH (t)	0.017	α: 2.10	1.21	0.064	180.0
		β: 2.88	1.08	0.070	
NCH···NF (t)	0.006	α: 0.84	0.87	0.034	143.6
		β: 0.68	1.05	0.034	
NCH···FN (t)	0.003	α: 0.40	1.19	0.027	158.8
		β: 0.41	1.55	0.032	
CNH···NH (t)	0.030	α: 3.74	1.24	0.086	180.0
		β: 5.13	1.10	0.095	
CNH···NF (t)	0.009	α: 1.52	0.92	0.047	138.5
		β: 1.01	1.09	0.042	
CNH···FN (t)	0.005	α: 0.91	1.15	0.041	135.7
		β: 0.49	0.91	0.028	
FH···PH (t)	0.012	α: 2.60	0.76	0.056	127.8
		β: 0.80	0.98	0.036	
FH···FP (t)	0.009	α: 1.85	1.09	0.057	150.0
		β: 1.28	1.57	0.057	
NCH···PH (t)	0.005	α: 0.89	0.76	0.033	138.2
		β: 0.45	0.95	0.026	
NCH···FP (t)	0.007	α: 0.96	1.44	0.047	163.0
		β: 1.43	1.54	0.059	
CNH···PH (t)	0.012	α: 1.90	0.79	0.049	133.3
		β: 0.86	0.99	0.037	
CNH···FP (t)	0.012	α: 2.28	1.20	0.066	153.2
		β: 1.97	1.57	0.071	

In all cases the charge is transferred from the HB acceptor (which is the electron donor) to the HB donor (HF, CNH, and NCH). Further inspection of the NBO second-order interaction energies shows that the charge is transferred by a $n_{HBA} \rightarrow \sigma^*_{HBD}$ donor−acceptor interaction. The charge transferred from one of the lone pairs, n_X, of the atom that accepts the HB (X in A−H···X−Y) to the closer A−H antibonding orbital, σ^*_{AH}, of the HB donor has been found to be fundamental in HB interactions.[24] In the case of the complexes formed by HB acceptors that are triplets (NH, NF, PH, and PF), two of these interactions were observed, one when analyzing the α-spin−orbitals and a parallel one when analyzing the *β*-spin−orbitals (see Table 6).

When describing the NBO analysis, Reed, Curtiss, and Weinhold[24] outlined the case of the NO−HF complexes where they explained the interactions in terms of what they referred to as "different hybrids for different spins" open-shell NBO description. They concluded that the *β*-spin set favors the linear structures, whereas the α-spin system favors bent (HXY ≈ 120°) structures. In the present study, we have found that in those complexes that are triplets (those with NH, NF, FN, PH, and FP), when the $\Delta E_{ij}^{(2)}$ corresponding to the *β*-spin set is larger than that of the α-spin set, the molecule is linear (see Table 8 for all the complexes with NH). In contrast, when the $\Delta E_{ij}^{(2)}$ of the α-spin set is larger than that of the *β*-spin set, the molecule is bent with HXY angles between 127.8 and 153.2° (see Table 8). However, there are two border cases that seem to establish the limit for the bending angle up to 155°. Complexes NCH···FN and NCH···FP, with HXY angles of 158.8 and 163.0°, show $\Delta E_{ij}^{(2)}$s very similar for both α- and *β*-spin sets, being a little larger than that corresponding to the *β*-spin set, which would imply a linear structure.

Depending on the group of the p.s. to which the HB acceptor atom belongs, different correlations can be established between the $\Delta E_{ij}^{(2)}$ values and the computed interaction energies, E_I, calculated at the B3LYP/6-311++G** level. This is consistent with the fact that $\Delta E_{ij}^{(2)}$s were computed at that level. Thus, for A−H···X−Y complexes the following equations were found:

$$\text{when X} = \text{B, Al,} \quad E_I = -(0.29 \pm 0.03)\Delta E_{ij}^{(2)}; \quad r^2 = 0.97,\ S_D = 0.83,\ n = 12 \quad (7)$$

$$\text{when X} = \text{N, P,} \quad E_I = -(0.95 \pm 0.16)\Delta E_{ij}^{(2)}; \quad r^2 = 0.96,\ S_D = 0.65,\ n = 9 \quad (8)$$

$$\text{when X} = \text{F,} \quad E_I = -(1.18 \pm 0.19)\Delta E_{ij}^{(2)}; \quad r^2 = 0.94,\ S_D = 1.10,\ n = 12 \quad (9)$$

Similarly, when comparing the charge transfer in the formation of the complex, ΔQ (calculated from the NP analysis), with the interaction energy and depending on the group of the p.s. to which the accepting atom belongs, we found the following correlations:

$$\text{when X} = \text{B, Al,} \quad E_I = -(70 \pm 5)\Delta Q; \quad r^2 = 0.99,\ S_D = 0.58,\ n = 12 \quad (10)$$

$$\text{when X} = \text{N, P,} \quad E_I = -(176 \pm 33)\Delta Q; \quad r^2 = 0.95,\ S_D = 0.72,\ n = 9 \quad (11)$$

$$\text{when X} = \text{F,} \quad E_I = -(400 \pm 45)\Delta Q; \quad r^2 = 0.97,\ S_D = 0.77,\ n = 12 \quad (12)$$

It can be noted that as one moves up the group of the p.s. (from group 13 to 15 to 17), the slope of both sets of regressions becomes more negative, from −0.29 to −0.95 to −1.18 in the case of $\Delta E_{ij}^{(2)}$ and from −70 to −176 to −400 in the case of ΔQ. This has been represented in Figure 4.

Electron Density and AIM. By use of the AIM approach, the electron density at the bond critical points (ρ_{BCP}), its Laplacian ($\nabla^2\rho_{BCP}$), and the energy density at the bond critical points (H_{BCP}) were evaluated for each bond in the monomers, protonated species, and HB complexes at the MP2/6-311++G** level. The results are shown in Tables 7 and 8. We have used H_{BCP} better than the Laplacian of the electron density to characterize the nature of the bonds studied because it is a more sensible index and therefore more appropriate for studying weak bonds.[25] Thus, whereas $\nabla^2\rho_{BCP}$ is usually positive in weak bonds, H_{BCP} can become negative in some HBs, showing the real strength of those bonds.

In the case of the monomers (see Table 7), large values of ρ_{BCP} with negative energy densities are observed for all the monomers except for AlF. This indicates the presence of "shared" interactions (usually referred to as covalent bonds). In the case of AlF, positive values of $\nabla^2\rho_{BCP}$s and H_{BCP} are obtained, indicating "closed-shell" interactions (usually referred to as ionic, hydrogen bond, or van der Waals interactions).

For the protonated species, the ρ_{BCP}s, $\nabla^2\rho_{BCP}$s, and H_{BCP}s are also gathered in Table 7. As expected, when covalently bonded molecules are protonated, the resulting H−X bonds are also covalent. When the weakly bonded AlF is protonated, two

TABLE 7: Electron Density (ρ_{BCP}, *e*/au^3), Laplacian ($\nabla^2\rho_{BCP}$, *e*/au^5), and Energy Density (H_{BCP}, Hartree/au^3) at the Bond Critical Points of the Monomers and Protonated Species Calculated at the MP2/6-311++G Level[a]**

				X−Y			interaction
	ρ_{BCP}	$\nabla^2\rho_{BCP}$	H_{BCP}	ρ_{BCP}	$\nabla^2\rho_{BCP}$	H_{BCP}	type[b]
BH				0.1799	−0.4506	−0.1961	S
BF				0.2148	1.5549	−0.1246	S
AlH				0.0736	0.2280	−0.0230	S
AlF				0.0885	0.8496	0.0153	C
NH(t)				0.3301	−0.4848	−0.4313	S
NF(t)				0.3464	−0.4848	−0.4266	S
PH(t)				0.1611	0.0383	−0.1563	S
PF(t)				0.1384	0.6264	−0.0810	S
HF	0.370	−2.836	−0.8039				S

	H−X			X−Y			interaction
[H−X-Y]$^+$	ρ_{BCP}	$\nabla^2\rho_{BCP}$	H_{BCP}	ρ_{BCP}	$\nabla^2\rho_{BCP}$	H_{BCP}	type[b]
[HBH]$^+$	0.2181	−0.7884	−0.2570	0.2181	−0.7884	−0.2570	S/S
[HBF]$^+$	0.2109	−0.7371	−0.2424	0.2711	1.8534	−0.2204	S/S
[HFB]$^+$	0.3223	−2.5785	−0.7129	0.0591	0.0277	−0.0220	S/S
[HAlH]$^+$	0.0927	0.3039	−0.0336	0.0927	0.3039	−0.0336	S/S
[HAlF]$^+$	0.0934	0.2986	−0.0343	0.1131	1.1676	0.0139	S/C
[HFAl]$^+$	0.3416	−2.7096	−0.7552	0.0216	0.0355	−0.0036	S/S
[HNH]$^+$	0.3064	−2.0195	−0.5386	0.3064	−2.0195	−0.5386	S/S
[HNF]$^+$	0.2846	−1.8442	−0.4917	0.4499	−1.1444	−0.7193	S/S
[HFN]$^+$	0.2997	−2.4206	−0.6605	0.1832	0.2404	−0.0982	S/S
[HPH]$^+$	0.1777	−0.1154	−0.1857	0.1777	−0.1154	−0.1857	S/S
[HPF]$^+$	0.1720	−0.2620	−0.1833	0.1734	1.0578	−0.0985	S/S
[HFP]$^+$	0.3267	−2.6236	−0.7249	0.0571	0.1037	−0.0179	S/S

[a] As a reference the values for HF are also given. [b] S = shared; C = closed-shell.

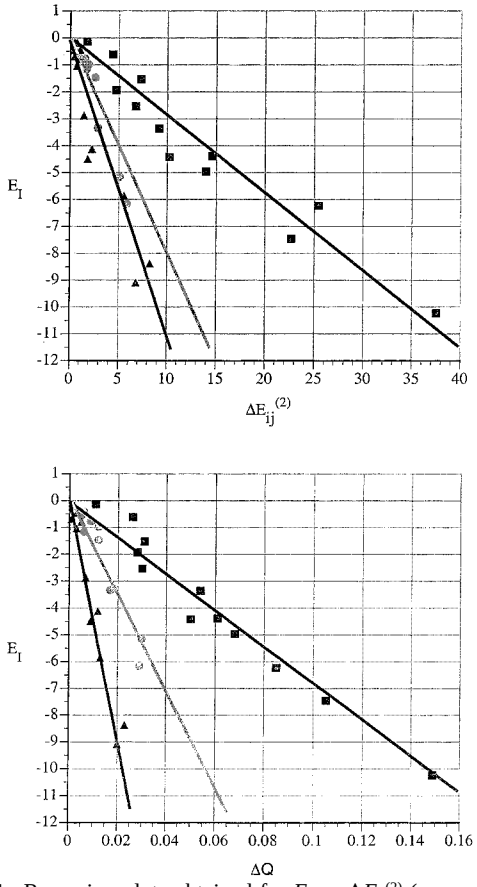

Figure 4. Regresion plots obtained for E_I vs $\Delta E_{ij}^{(2)}$ (upper part) and vs ΔQ (lower part) for all the HB complexes studied.

covalent bonds (H−Al and H−F) are formed. The other ones, Al−F(H) and F···Al(H), become shared or remain as closed-shell interactions (see Table 7).

Henceforth, we will refer to van der Waals interactions as those with $\rho_{BCP} \approx 10^{-3}$ au and HBs as those with $\rho_{BCP} \approx 10^{-2}$ au. In all the complexes studied, BCPs were found corresponding to HBs or to van der Waals interactions. The results obtained are shown in Table 8. In the HB complexes formed by

TABLE 8: Electron Density (ρ_{BCP}, *e*/au^3), Laplacian ($\nabla^2\rho_{BCP}$, *e*/au^5), and Energy Density (H_{BCP}, Hartree/au^3) at the Bond Critical Points of the HB Complexes

	H···X			X−Y		
A−H···X−Y	ρ_{BCP}	$\nabla^2\rho_{BCP}$	H_{BCP}	ρ_{BCP}	$\nabla^2\rho_{BCP}$	H_{BCP}
FH···BH	0.0308	0.0492	−0.0034	0.1866	−0.4815	−0.2066
FH···BF	0.0214	0.0466	0.0002	0.2219	1.6147	−0.1332
FH···FB	0.0074	0.0367	0.0021	0.2069	1.5006	−0.1145
NCH···BH	0.0105	0.0240	0.0010	0.1836	−0.4701	−0.2018
NCH···BF	0.0078	0.0189	0.0009	0.2188	1.5882	−0.1296
NCH···FB	0.0049	0.0206	0.0009	0.2093	1.5166	−0.1176
CNH···BH	0.0218	0.0395	−0.0004	0.1861	−0.4813	−0.2059
CNH···BF	0.0151	0.0343	0.0010	0.2215	1.6089	−0.1330
CNH···FB	0.0075	0.0342	0.0017	0.2067	1.4977	−0.1142
FH···AlH	0.0121	0.0172	0.0003	0.0759	0.2432	−0.0236
FH···AlF	0.0068	0.0118	0.0005	0.0906	0.8798	0.0156
FH···FAl	0.0295	0.1408	0.0023	0.0834	0.7775	0.0140
NCH···AlH	0.0060	0.0099	0.0002	0.0751	0.2380	−0.0235
NCH···AlF	0.0036	0.0069	0.0002	0.0900	0.8717	0.0155
NCH···FAl	0.0174	0.0751	0.0023	0.0853	0.7988	0.0141
CNH···AlH	0.0101	0.0141	0.0002	0.0760	0.2435	−0.0237
CNH···AlF	0.0062	0.0103	0.0002	0.0908	0.8830	0.0156
CNH···FAl	0.0272	0.1212	0.0021	0.0828	0.7688	0.0139
FH···NH	0.0239	0.0942	0.0026	0.3316	−1.5566	−0.4485
FH···NF	0.0078	0.0323	0.0021	0.3561	−0.5484	−0.4531
FH···FN	0.0111	0.0514	0.0022	0.3351	−0.4183	−0.3975
NCH···NH	0.0111	0.0404	0.0021	0.3310	−1.5228	−0.4410
NCH···NF	0.0052	0.0179	0.0008	0.3527	−0.5255	−0.4436
NCH···FN	0.0056	0.0241	0.0010	0.3381	−0.4365	−0.4058
CNH···NH	0.0197	0.0740	0.0028	0.3314	−1.5531	−0.4476
CNH···NF	0.0076	0.0295	0.0017	0.3567	−0.5521	−0.4544
CNH···FN	0.0106	0.0466	0.0019	0.3343	−0.4125	−0.3958
FH···PH	0.0081	0.0233	0.0014	0.1628	0.0354	−0.1586
FH···FP	0.0220	0.1102	0.0032	0.1304	0.5502	−0.0758
NCH···PH	0.0055	0.0149	0.0007	0.1623	0.0349	−0.1579
NCH···FP	0.0132	0.0575	0.0021	0.1329	0.5740	−0.0774
CNH···PH	0.0083	0.0223	0.0010	0.1630	0.0349	−0.1589
CNH···FP	0.0202	0.0947	0.0028	0.1299	0.5461	−0.0756

covalently bonded monomers, those bonds remain covalent (large ρ_{BCP} and negative H_{BCP}s). Similarly, those monomers with closed-shell interactions remain bonded in a similar way within the HB complexes.

In agreement with the energy results, NH, FAl, and FP form HB complexes with any of the HB donors, showing values of ρ_{BCP} of around 10^{-2} au and positive H_{BCP}s (see Table 8). The case of BH is more interesting, since it forms almost a covalent bond with the strongest acids FH and CNH (negative but small H_{BCP}s). Yet, BF, AlH, and FN form HB complexes only with CNH and HF (see Table 8), and they form van der Waals complexes with NCH (ρ_{BCP} of around 10^{-3} au). The rest of the bases, NF, PH, AlF, and FB form van der Waals complexes with all of the acids used (see Table 8). These three groups are very similar to those three groups made in terms of the function of the interaction energy. Thus, taking into account both energy and electron density, it can be established that, independently of the acid used, the diatomic molecules BH, NH, FAl, and FP are good HB acceptors. Then there is an intermediate group formed by BF, AlH, and FN that can be good, medium, or poor HB acceptors depending on the donor used. And the last group is formed by those molecules (NF, PH, AlF, and FB) that, even though interacting with HB donors, form rather weak complexes. In the mentioned intermediate group there are two molecules with unexpected electron density compared with the stability of the complex. On one hand, BF provides HB complexes with large interaction energies (i.e., at the MP2/6-311++G** level; FH···BF is −4.62, CNH···BF is −4.32, and NCH···BF is −2.44 kcal/mol; see Table 3), but the electron density at the bond critical point of these complexes varies with the acid (FH···BF is 0.0214, CNH···BF is 0.0151, and NCH···BF is 0.0078 au; see Table 8). On the other hand, the HB complexes with FN show medium to small ρ_{BCP}s (FH···FN is 0.0111, CNH···FN is 0.0106, and NCH···FN is 0.0056 au; see Table 8), whereas the stability of those complexes was very low (i.e., at the MP2/6-311++G** level, FH···FN is −0.80, CNH···FN is −0.89, and NCH···FN is −0.44 kcal/mol; see Table 3). Overall, considering the electron and energy densities and the Laplacian of the electron density of all these HB complexes, most of them are at least as strong as the FH···FH dimer, which at the MP2/6-311++G** level shows $\rho_{BCP} = 0.021$, $\nabla^2\rho_{BCP} = 0.0990$, and $H_{BCP} = 0.0029$.[26]

In general, the electron density at the bond critical point of the HB acceptors increases when the monomer is protonated or forms an HB complex, and the acceptor is B, Al, N, or P. However, when the atom being protonated or accepting the HB is F, the ρ_{BCP} diminishes. The exception is $[HNH]^+$ in the case of the protonated species. This tendency is also observed in the bond distances of the diatomic molecules. Thus, the bond distance of the HB acceptors always increases when the molecule is protonated or forms an HB complex, when the accepting atom belongs to groups 13 or 15 of the p.s. When the molecule is protonated or forms the HB complex by the fluoride, the bond distance of the monomer diminishes. This effect was previously found by Alcamí et al.[27] in the sense that the protonation or HB formation depends on the relative electronegativity of the atoms forming the bond. Thus, when protonation (or hydrogen association in a HB) takes place at the most electronegative atom (for instance, F in FX molecules), the bond becomes significantly weaker. In contrast, if protonation takes place at the less electronegative atom (X in FX molecules), the bond becomes reinforced. Furthermore, and as we found in previous studies,[28] a direct relation exists between the ρ_{BCP} of the H···X bond and that of the HB distance.

Conclusions

Taking into account that the calculated H···X distances in an HB complex A−H···X−Y depend not only on the strength of the HB interaction but also on the nature of the acceptor atom X, a relative order of strength of the HB acceptors can be established relative to that acceptor atom independent of the acid fragment. Thus, when X = F, the H···F distances are FAl < FP < FN < FB. When X = N, the H···N distances are NH < NF. When X = B, the H···B distances are BH < BF. And when X= Al, the H···Al distances are AlH < AlF. These geometry results are in agreement with the MP2 interaction energies E_{I+BSSE} gathered in Table 3 and in Figure 1 where one observes that the order in stability of the HB complexes follows a reverse trend from that of the H···X distances: FAl > BH > NH > BF > FP > AlH > PH > FN > AlF > NF > FB (the exception is made for PH, with a relative stability versus any of the HB donors that is contrary to the HB distance obtained for each complex).

The use of principal component analysis allows for the expression of E_I as a function of acidity or basicity and the softness of the molecules involved in the HB complexes following Pearson's model. According to all our results of energy, electron density, and PCA, we can conclude that for the three acids used here, FH and CNH have similar acidity and they are more acidic than NCH. Regarding the bases used for the study, those more basic are FAl > BH > NH > BF > FP, and their strength seems to be independent of the acid used. For AlH the basicity depends on the acid utilized. And the worst bases, independent of the acid used, are PH > FN > AlF > NF > FB.

Thus, leaving apart the FY (Y = B, N, Al, P) derivatives, which are not directly the objective of our work, it seems that BY (group 13, first row of the p.s.) derivatives are very good HB acceptors. However, AlY and PY (second row of the p.s.) range from not very good to bad HB acceptors, whereas NY (group 15, first row of the p.s.) can be a strong base when Y = H and a weak one when Y = F.

Acknowledgment. The authors thank the Spanish DGICYT (Project No. SAF 97-0044-C02) and the EU network "Location and Transfer of Hydrogen" (No. CHRX CT 940582) for financial support. They also thank Dr. E. Elguero for suggesting the use of PCA, Dr. R. S. Chari for technical support in the preparation of this manuscript, and Dr. Nguyen and the referees for their constructive suggestions.

References and Notes

(1) March, J. *Advanced Organic Chemistry*, 4th ed.; John Wiley and Sons: New York, 1992.

(2) (a) Ehlers, A. W.; Baerends, J.; Bickelhaupt, F. M.; Radius, U. *Chem Eur J.* **1998**, *4*, 210. (b) Bickelhaupt, F. M.; Radius, U.; Ehlers, A. W.; Hoffmann, R.; Baerends, J. *New J. Chem.* **1998**, 1.

(3) Alkorta, I.; Elguero, J. *J. Phys. Chem.* **1996**, *100*, 19367.

(4) Frisch, M. J.; Trucks, G. W.; Schlegel, H. B.; Gill, P. M. W.; Johnson, B. G.; Robb, M. A.; Cheeseman, J. R.; Keith, T.; Petersson, G. A.; Montgomery, J. A.; Raghavachari, K.; Al-Laham, M. A.; Zakrzewski, V. G.; Ortíz, J. V.; Foresman, J. B.; Peng, C. Y.; Ayala, P. Y.; Chen, W.; Wong, M. W.; Andres, J. L.; Replogle, E. S.; Gomperts, R.; Martin, R. L.; Fox, D. J.; Binkley, J. S.; Defrees, D. J.; Baker, J.; Stewart, J. P.; Head-Gordon, M.; González, C.; Pople, J. A. *Gaussian 94*, revision E.2; Gaussian, Inc.: Pittsburgh, PA, 1995.

(5) Becke, A. D. *J. Chem. Phys.* **1993**, *98*, 5648.

(6) Hariharan, P. A.; Pople, J. A. *Theor. Chim. Acta* **1973**, *28*, 213.

(7) Krishnam, R.; Binkley, J. S.; Seeger, R.; Pople, J. A. *J. Chem. Phys.* **1984**, *80*, 3265.

(8) Møller, C.; Plesset, M. S. *Phys. Rev.* **1934**, *46*, 618.

(9) Curtiss, L. A.; Raghavachari, K.; Trucks, G. W.; Pople, J. A. *J. Chem. Phys.* **1991**, *94*, 7221.

(10) Hegarty, D.; Robb, M. A. *Mol. Phys.* **1979**, *38*, 1795.

(11) Boys, S. B.; Bernardi, F. *Mol. Phys*. **1970**, *19*, 553.
(12) Glendening, A. E.; Reed, A. E.; Carpenter, J. E.; Weinhold, F. *NBO*, version 3.1.
(13) Weinhold, F. Personal communication.
(14) Bader, R. F. W. *Atoms in Molecules. A Quantum Theory*; Oxford University: New York, 1990.
(15) Bieger-Konig, F. W.; Bader, R. F. W.; Tang, T. H. J. *J. Comput. Chem*. **1982**, *3*, 317.
(16) Boldyrev, A. I.; Gonzales, N.; Simons, J. *J. Phys. Chem.* **1994**, *98*, 9931 and references therein.
(17) Hehre, W. J.; Radom, L.; Schleyer, P. v. R.; Pople, J. A. *Ab Initio Molecular Orbital Theory*; John Wiley & Sons: New York, 1986; p 352.
(18) (a) McKellar, A. R. W.; Bunker, P. R.; Sears, T. J.; Evenson, K. M.; Saykally, R. J.; Langhoff, S. R. *J. Chem. Phys*. **1983**, *79*, 5251. (b) Sears, T. J.; Bunker, P. R. *J. Chem. Phys*. **1983**, *79*, 5265 and references therein.
(19) Brugers, P. D.; Holmes, J. L.; Mommers, A. A. *J. Am. Chem. Soc*. **1985**, *107*, 1099.
(20) (a) Samanta, U.; Chakrabarti, P.; Chandrasekhar, J. *J. Phys. Chem. A* **1998**, *102*, 8964. (b) Dunbar, R. C. *J. Phys. Chem. A* **1998**, *102*, 8946.
(21) Alkorta, I.; Rozas, I.; Elguero, J. *Chem. Soc. Rev*. **1998**, *27*, 155.
(22) Pearson, R. G. *Hard and Soft Acids and Bases*; Dowden, Hutchinson & Ross, Inc.: Stroudsburg, PA, 1973. Pearson, R. G. The Influence of the Reagent on Organic Reactivity. In *Advances in Linear Free Energy Relationships*; Chapman, N. B., Shorter, J., Eds.; Plenum Press: New York, 1972; p 281. Ho, T. L. *Hard and Soft Acids and Bases Principle in Organic Chemistry*; Academic Press: New York, 1977.
(23) (a) Legon, A. C.; Millen, D. J. *J. Am. Chem. Soc*. **1987**, *109*, 356. (b) Legon, A. C.; Millen, D. J. *J. Chem. Soc., Chem. Commun*. **1987**, 986. (c) Legon, A. C. *Chem. Commun*. **1998**, 2585.
(24) Reed, A. E.; Curtiss, L. A.; Weinhold, F. *Chem. Rev.* **1988**, *88*, 899.
(25) Koch, W.; Frenking, G.; Gauss, J.; Cremer, D.; Collins, J. R. *J. Am. Chem. Soc.* **1987**, 5917.
(26) Alkorta, I.; Rozas, I.; Elguero, J. *J. Phys. Chem. A* **1998**, *102*, 9278.
(27) Alcamí, M.; Mó, O.; Yáñez, M.; Abboud, J.-L. M.; Elguero, J. *Chem. Phys. Lett.* **1990**, *172*, 471.
(28) (a) Alkorta, I.; Elguero, J. *Struct. Chem.*, in press. (b) Alkorta, I.; Rozas, I.; Elguero, J. *Struct. Chem.* **1998**, *9*, 243.